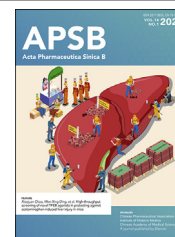




Chinese Pharmaceutical Association  
Institute of Materia Medica, Chinese Academy of Medical Sciences

Acta Pharmaceutica Sinica B

[www.elsevier.com/locate/apsb](http://www.elsevier.com/locate/apsb)  
[www.sciencedirect.com](http://www.sciencedirect.com)



ORIGINAL ARTICLE

# Phosphatidic acid-enabled MKL1 contributes to liver regeneration: Translational implication in liver failure



Jiawen Zhou<sup>a,†</sup>, Xinyue Sun<sup>a,†</sup>, Xuelian Chen<sup>a</sup>, Huimin Liu<sup>a</sup>,  
Xiulian Miao<sup>b</sup>, Yan Guo<sup>b</sup>, Zhiwen Fan<sup>c</sup>, Jie Li<sup>d,e,\*</sup>, Yong Xu<sup>a,b,\*</sup>,  
Zilong Li<sup>a,b,\*</sup>

<sup>a</sup>State Key Laboratory of Natural Medicines, Department of Pharmacology, China Pharmaceutical University, Nanjing 211198, China

<sup>b</sup>Institute of Biomedical Research, Liaocheng University, Liaocheng 252200, China

<sup>c</sup>Department of Pathology, Affiliated Nanjing Drum Tower Hospital of Nanjing University Medical School, Nanjing 210008, China

<sup>d</sup>Department of Infectious Diseases, Nanjing Drum Tower Hospital Affiliated with Nanjing University Medical School, Nanjing 210008, China

<sup>e</sup>Institute of Viruses and Infectious Diseases, Nanjing University, Nanjing 210008, China

Received 25 May 2023; received in revised form 5 September 2023; accepted 13 September 2023

## KEY WORDS

Liver failure;  
Liver regeneration;  
Transcription regulation;  
Transcription factor;  
Hepatocytes;  
Phosphatidic acid;  
Phospholipase d2;  
Translational medicine

**Abstract** Liver regeneration following injury aids the restoration of liver mass and the recovery of liver function. In the present study we investigated the contribution of megakaryocytic leukemia 1 (MKL1), a transcriptional modulator, to liver regeneration. We report that both MKL1 expression and its nuclear translocation correlated with hepatocyte proliferation in cell and animal models of liver regeneration and in liver failure patients. Mice with MKL1 deletion exhibited defective regenerative response in the liver. Transcriptomic analysis revealed that MKL1 interacted with E2F1 to program pro-regenerative transcription. MAPKAPK2 mediated phosphorylation primed MKL1 for its interaction with E2F1. Of interest, phospholipase d2 promoted MKL1 nuclear accumulation and liver regeneration by catalyzing production of phosphatidic acid (PA). PA administration stimulated hepatocyte proliferation and enhanced survival in a MKL1-dependent manner in a pre-clinical model of liver failure. Finally, PA levels was detected to be positively correlated with expression of pro-regenerative genes and inversely correlated with liver injury in liver failure patients. In conclusion, our data reveal a novel mechanism whereby

\*Corresponding authors.

E-mail addresses: [lzl1114@cpu.edu.cn](mailto:lzl1114@cpu.edu.cn) (Zilong Li), [yjxu@cpu.edu.cn](mailto:yjxu@cpu.edu.cn) (Yong Xu), [lijier@sina.com](mailto:lijier@sina.com) (Jie Li).

<sup>†</sup>These authors made equal contributions to this work.

Peer review under the responsibility of Chinese Pharmaceutical Association and Institute of Materia Medica, Chinese Academy of Medical Sciences.

<https://doi.org/10.1016/j.apsb.2023.10.011>

2211-3835 © 2024 The Authors. Published by Elsevier B.V. on behalf of Chinese Pharmaceutical Association and Institute of Materia Medica, Chinese Academy of Medical Sciences. This is an open access article under the CC BY-NC-ND license (<http://creativecommons.org/licenses/by-nc-nd/4.0/>).

MKL1 contributes to liver regeneration. Screening for small-molecule compounds boosting MKL1 activity may be considered as a reasonable approach to treat acute liver failure.

© 2024 The Authors. Published by Elsevier B.V. on behalf of Chinese Pharmaceutical Association and Institute of Materia Medica, Chinese Academy of Medical Sciences. This is an open access article under the CC BY-NC-ND license (<http://creativecommons.org/licenses/by-nc-nd/4.0/>).

## 1. Introduction

A key metabolic and detoxification organ, the liver is susceptible to a wide range of injurious stimuli that include trauma, ischemia, hepatotoxic substances, pathogens, influx of excessive nutrients, or a combination of the above<sup>1</sup>. The loss of liver parenchyma following injury, *via* several different cell death programs, parallels the impairment of key liver functions and disrupts the internal homeostasis jeopardizing the well-being of the affected individuals. On the other hand, liver injury can be compensated for and counterbalanced by the intrinsic regenerative capacity of hepatocytes, having withdrawn temporarily from active cell cycling after the completion of development, which serves to offset, to varying extents, injury-induced loss of liver mass<sup>2</sup>. Therefore, full-fledged robust liver regeneration aids the normalization of both hepatic architecture and function. On the contrary, compromised or defective liver regeneration is usually synonymous with liver failure that necessitates organ transplantation, an undesirable outcome compounded by donor availability and host-graft rejection<sup>3</sup>.

A vast network of signaling cascades coordinate the regenerative response of hepatocytes following injury by forming extensive crosstalk that converges in the nucleus. A host of transcription factors, guided by the pro-regenerative cues, program the dynamic changes in cellular transcriptome fueling hepatocyte regeneration<sup>4</sup>. Wnt signaling, for instance, represents one of the best characterized prototypical pro-regenerative pathways in the liver: absent the Wnt ligand, the downstream effector  $\beta$ -catenin becomes ubiquitinated and degraded leaving hepatocytes in a quiescent state; stimulated by a pro-regenerative cue,  $\beta$ -catenin sheds the polyubiquitination modification and translocates into the nucleus where it functions a key transcriptional modulator to facilitate hepatocyte re-population<sup>5</sup>. The Hippo/YAP pathway is another classic example of pro-regenerative signaling cascades. Stimulated by a ligand whose identity remains mysterious, YAP/TAZ undergo de-phosphorylation, escape from proteasomal degradation, and migrate into the nucleus to function as co-activators for the TEAD transcription factors mediating pro-proliferative transcription<sup>6</sup>. Consistently, deletion or inhibition of the pro-regenerative signaling molecules and transcription factors (TFs) impairs liver regeneration *in vivo*<sup>7</sup>. From a transcriptional perspective, liver regeneration is orchestrated by orderly recruitment of TFs to the chromatin. Because naïve chromatin is unfriendly for TF binding, a sophisticated mechanism must be in place to rewire the chromatin and alter accessibility. A recent report by Wang et al.<sup>8</sup> portrays a genomewide blueprint of altered chromatin accessibility in re-populating hepatocytes. Tens of thousands of chromatin regions undergo active remodeling, as suggested by the Wang et al.'s study, that contribute to the dynamic unmasking/masking of binding sites for key TFs involved in liver regeneration.

Megakaryocytic leukemia 1 (MKL1), also known as myocardin-related transcription factor A (MRTF-A), was initially identified as

a co-factor for serum response factor (SRF) with a ubiquitous expression pattern<sup>9</sup>. CHIP-seq combined with single locus-based analyses have provided support for a model wherein MKL1 dictates signal-responsive transcription events by coordinating with a wide range of sequence-specific TFs including AP-1, SMAD, STAT, YAP/TEAD, and NF- $\kappa$ B<sup>10,11</sup>. Recent investigations have accumulated mounting evidence to implicate MKL1 in the regulation of cellular proliferation in the context of carcinogenesis<sup>12,13</sup>. For instance, it has been demonstrated that MKL1 is preferentially localized to the nucleus in certain types of hepatocellular carcinoma (HCC) cells to fuel cancerous proliferation<sup>14</sup>. Conversely, MKL1 deletion diminishes malignant HCC growth by committing HCC cells to senescence<sup>15</sup>. Thus far, there has been no direct proof to validate or dispute the notion that MKL1 may play a role in liver regeneration. Here we present data to show that MKL1 is essential for liver regeneration *in vivo* by orchestrating the pro-regenerative transcriptional program.

## 2. Materials and methods

### 2.1. Animals

All the animal experiments were reviewed and approved by the China Pharmaceutical University Ethics Committee on Humane Treatment of Laboratory Animals. The MKL1 knockout mice<sup>16</sup> have been described previously. C57BL/6 mice were purchased from GemPharmatech (Nanjing, China). Global MKL1 knockout mice (KO), in which exons 9 through 14 were deleted by homologous recombination, have been described previously<sup>16</sup>. To generate liver-specific MKL1 knockout mice, *Mkl1*<sup>fl/fl</sup> mice<sup>17</sup>, in which exons 9 through 14 were floxed, were crossbred with *Alb-Cre* mice<sup>18</sup>. The F1 offspring (*Mkl1*<sup>fl/+</sup>; *Alb-Cre*) was crossbred to the *Mkl1*<sup>fl/fl</sup> mice and the resulting Cre<sup>+</sup> F2 progenies (*Mkl1*<sup>fl/fl</sup>; *Alb-Cre*) were designated as the MKL1<sup>LKO</sup> mice whereas the Cre<sup>-</sup> F2 progenies (*Mkl1*<sup>fl/fl</sup>) were designated as the WT mice.

To investigate liver regeneration, two animal models were exploited. In the first model, partial hepatectomy (PHx) was performed in 6-week male mice as previously described<sup>19,20</sup>. For 2/3 PHx, the mice were anesthetized with 2% isoflurane and a midline incision was created to expose the xiphoid process. Place a silk thread on the base of the left lateral lobe, tie the two ends of the suture over the top of the left lateral lobe, and remove the tied lobe just above the suture with a microsurgical scissor. Then place a thread for the second knot between the stump and the median lobe and remove the tied median lobe above the suture. For 4/5 PHx, the caudate lobe, in addition to the median and left lateral lobe, was surgically removed. After the surgery, the mice were placed on a heating pad for recovering before being transferred back to the cage. In the second model, acetaminophen (PHx) was administered in 8-week male mice as previously described<sup>21,22</sup>. Briefly, the mice were fasted overnight (12–16 h) with free access to water. The next day, APAP dissolved in warm saline was

administered *via* intraperitoneal injection at 300 mg/kg (non-lethal) or 800 mg/kg (lethal). For administration of phosphatidic acid (PA), egg PA extract (Avanti Polar Lipids) was dissolved in at 10% DMSO/PBS pre-heated to 80 °C to achieve a uniform solution, cooled to body temperature right before administration, and injected intraperitoneally at 20 mg/kg daily for three days prior to the PHx procedure. In certain experiments, the mice were subjected to the sham surgery or injected with saline and sacrificed immediately after the procedure; samples collected from the mice were labeled “0 h”. In certain experiments, *Pld2*-targeting shRNA (GGCGAACAGUUCUGAACAAATT) was placed downstream of the human thyroxin binding globulin (TBG) promoter, packed into AAV8, and injected into mice *via* tail vein ( $1 \times 10^{11}$  GC/mouse) two weeks prior to the PHx procedure.

## 2.2. Cell culture, plasmids, transient transfection, and reporter assay

Primary murine hepatocytes were isolated and maintained in DMEM supplemented with 10% FBS as previously described<sup>23,24</sup>. HepG2 and HEK293 cells were maintained in DMEM supplemented with 10% FBS. MKL1 promoter-luciferase construct was generated by amplifying genomic DNA spanning the proximal promoter and the first exon (−1585/+114) of *MKL1* gene and ligating into a pGL3-basic vector (Promega). FLAG-tagged MKL1<sup>25</sup> and GFP-tagged E2F1<sup>26</sup> constructs have been previously described. Truncation or point mutation was introduced using a QuikChange kit (Thermo Fisher) and verified by direct sequencing. Small interfering RNAs were purchased from Dharmacon: siPld2#1, 5′-GGUUGAGUCCUGAAAUUUATT-3′, and siPld2#2, 5′-GGAUGUUGGAGUGGUUUAATT-3′. Transient transfection was performed with Lipofectamine LTX (for primary hepatocytes), Lipofectamine 3000 (for HepG2 and HEK293 cells) or Lipofectamine RNAiMax (for all siRNAs). Cells were harvested 24 h after transfection and reporter activity was measured using a luciferase reporter assay system (Promega) as previously described<sup>27</sup>.

## 2.3. RNA isolation and real-time PCR

RNA was extracted with the RNeasy RNA isolation kit (Qiagen) as previously described<sup>28</sup>. Reverse transcriptase reactions were performed using a SuperScript First-strand Synthesis System (Invitrogen). Real-time PCR reactions were performed on an ABI Prism 7500 system with the following primers:

Mouse *Mkl1*, 5′-AGGACCGAGGACTATTTGAAACG-3′ and 5′-CCACAATGATAGCCTCCTTCAG-3′;  
 Human *MKL1*, 5′-ATGCCGCCTTTGAAAAGTCCA-3′ and 5′-TCTTCCGTTTGAGATAGTCTCT-3′;  
 Mouse *Ccna2*, 5′-AAGAGAATGTCAACCCCGAAAAA-3′ and 5′-ACCCGTCGAGTCTTGAGCTT-3′;  
 Human *CCNA2*, 5′-CGCTGGCGGTACTGAAGTC-3′ and 5′-GAGGAACGGTGACATGCTCAT-3′;  
 Mouse *Ccnd1*, 5′-GCGTACCCTGACACCAATCTC-3′ and 5′-ACTTGAAGTAAGATACGGAGGGC-3′;  
 Human *CCND1*, 5′-GCTGCGAAGTGGAAACCATC-3′ and 5′-CCTCCTTCTGCACACATTTGAA-3′;  
 Mouse *Pcna*, 5′-TTTGAGGCACGCCTGATCC-3′ and 5′-GAGACGTGAGACGAGTCCAT-3′;  
 Human *PCNA*, 5′-CCTGCTGGGATATTAGCTCCA-3′ and 5′-CAGCGGTAGGTGTCAAGC-3′;

Mouse *Myc*, 5′-CTTCTCTCCGTCCTCGGATTCT-3′ and 5′-GAAGGTGATCCAGACTCTGACCTT-3′;  
 Mouse *Cdc25*, 5′-GCAGCAGCGTTAATTCATCTACT-3′ and 5′-GGCCGAAGAGAGTTTGTCCAC-3′;  
 Mouse *Ccnb1*, 5′-CAATTATCGGAAGTGTCCGATCA-3′ and 5′-CTGGTGAACGACTGAACTCCC-3′;  
 Human *CCNB1*, 5′-GCGTGTGGACATTAGCTCCCG-3′ and 5′-GCGCTCCATAAGTTTCTCAGAG-3′;  
 Mouse *Ccne1*, 5′-CTCCGACCTTTCAGTCCGC-3′ and 5′-CAGTCTTGTCAATCTTGGCA-3′;  
 Mouse *Ccne2*, 5′-ATGTCAAGACGCAGCCGTTTA-3′ and 5′-GATTCCTCCAGACAGTACA-3′;  
 Mouse *Cdk1*, 5′-ATGTGCGACCTCATTGAACCG-3′ and 5′-GAAACTCTCGACAAAAGTTCTCC-3′;  
 Mouse *Pld1*, 5′-CATCGACAGCACCTCCAAC-3′ and 5′-GAGTTCTCCCACTCCGGTCT-3′;  
 Mouse *Pld2*, 5′-TGGGTGACCCCTCTGAACCTGT-3′ and 5′-GTCCAGCTGCACCCAGTCCT-3′.

Ct values of target genes were normalized to the Ct values of housekeeping control gene (18s, 5′-CGCGGTTCTATTTTGTGGT-3′ and 5′-TCGTCTTCGAAACTCCGACT-3′ for both human and mouse genes) using the  $\Delta\Delta$ Ct method and expressed as relative mRNA expression levels compared to the control group which is arbitrarily set as 1<sup>29,30</sup>.

## 2.4. Protein extraction and Western blot

Whole cell lysates were obtained by re-suspending cell pellets in RIPA buffer (50 mmol/L Tris pH 7.4, 150 mmol/L NaCl, 1% Triton X-100) with freshly added protease inhibitor (Roche) as previously described<sup>31,32</sup>. Nuclear proteins were extracted using the NE-PER Kit (Pierce) following manufacturer’s recommendation<sup>33</sup>. 30  $\mu$ g of protein were loaded in each lane and separated by 8% PAGE-SDS gel with all-blue protein markers (Bio-Rad). Proteins were transferred to nitrocellulose membranes (Bio-Rad) in a Mini-Trans-Blot Cell (Bio-Rad). The membranes were blocked with 5% fat-free milk powder in Tris-buffered saline (TBS) at room temperature for half an hour and then incubated with the primary antibodies listed in [Supporting Information Table S1](#) at 4 °C overnight. The next day, the membranes were washed with TBS and incubated with HRP conjugated anti-rabbit secondary antibody (Thermo Fisher, 61–6520, 1:5000) or anti-mouse secondary antibody (Thermo Fisher, 31464, 1:5000) for 1 h at room temperature as previously described<sup>34</sup>. For densitometrical quantification, densities of target proteins were normalized to those of  $\beta$ -actin. Data are expressed as relative protein levels compared to the control group which is arbitrarily set as 1.

## 2.5. Histology

Histological analyses were performed essentially as described before. Paraffin sections were stained with were blocked with 10% normal goat serum for 1 h at room temperature and then incubated with anti-Ki67 (Abcam, 1:200), or anti-BrdU (Abcam, 1:200) antibodies. Staining was visualized by incubation with anti-rabbit secondary antibody and developed with a streptavidin-horseradish peroxidase kit (Pierce) for 20 min. Pictures were taken using an Olympus IX-70 microscope. Quantifications were performed with Image J.

## 2.6. RNA sequencing and data analysis

Total RNA was extracted using the TRIzol reagent according to the manufacturer's protocol. RNA purity and quantification were evaluated using the NanoDrop 2000 spectrophotometer (Thermo Scientific, USA). RNA integrity was assessed using the Agilent 2100 Bioanalyzer (Agilent Technologies, Santa Clara, CA, USA). Then the libraries were constructed using TruSeq Stranded mRNA LT Sample Prep Kit (Illumina, San Diego, CA, USA) according to the manufacturer's instructions and sequenced on an Illumina HiSeq X Ten platform and 150 bp paired-end reads were generated. Raw data (raw reads) of fastq format were firstly processed using Trimmomatic and the low quality reads were removed to obtain the clean reads. The clean reads were mapped to the mouse genome (*Mus musculus*.GRCm38.99) using HISAT2. FPKM of each gene was calculated using Cufflinks, and the read counts of each gene were obtained by HTSeqcount. Differential expression analysis was performed using the DESeq (2012) R package. *P* value < 0.05 and fold change >2 was set as the threshold for significantly differential expression. Hierarchical cluster analysis of differentially expressed genes (DEGs) was performed to demonstrate the expression pattern of genes in different groups and samples. GO enrichment and KEGG pathway enrichment analysis of DEGs were performed respectively using R based on the hypergeometric distribution.

## 2.7. ATAC-seq experiment and data processing

ATAC-seq was performed using Active Motif ATAC-Seq Kit (Active Motif, 53150) according to manufacturer's instruction. Briefly, 20 mg tissue was minced with razor blade to the size of 1 mm<sup>2</sup> in cold PBS, re-suspended in 1 mL Lysis Buffer, and transferred to 1 mL dounce homogenizer for homogenization on ice. Tissue lysates were filtered through a 40 µm cell strainer (Falcon, 352340). 100,000 nuclei were aliquoted and centrifuged at 500×*g* at 4 °C for 5 min. The nuclei pellets were re-suspended in 50 µL Transposition Master Mix and incubated at 37 °C for 30 min in a thermomixer set at 800 rpm (Eppendorf ThermoMixer C, Eppendorf, Enfield, CT, USA). Transposed DNA was purified with SPRI beads and eluted in 35 µL Elution Buffer. Library was generated using Q5 High-Fidelity DNA Polymerase and sequenced on an Illumina X10 platform with PE150 strategy. Raw sequences were adapter-trimmed and mapped to hg38 (or mm10, etc.) using bwa. PCR duplicates were removed using Picard. Peak calling was performed by MACS2 with parameter (*f* = BAMPE; *nomodel*; *shift* = -100; *extsize* = 200; *q* = 0.05) and annotated by HOMER. Consensus peaks regions were identified between samples by Bedtools and counted intensity by featureCounts. "DESeq2" package in R was used to identify the differential peaks. Pearson correlation was calculated based on all the peaks by deeptools. Motif discovery was performed by HOMER. TSS/TES/Genebody enrichment was calculated by deeptools. "ClusterProfiler" package in R was used to perform the GO enrichment and KEGG pathway enrichment of differential peaks.

## 2.8. Chromatin immunoprecipitation (ChIP)

ChIP and Re-ChIP assays were performed essentially as described before using an EZ-Magna ChIP kit (Millipore). Briefly, cells ( $1 \times 10^7$ ~10 reactions) were cross-linked with 1% freshly prepared formaldehyde at room temperature for 10 min. Cells were washed with PBS and re-suspended in cell lysis buffer and then

nuclear lysis buffer to extract chromatin per vendor's instruction. The resulting material was then sonicated to create appropriately sized (200–500 bp) chromatin fragments using a Bioruptor (Diagenode). For liver tissue ChIP, we used a Magna ChIP G Tissue kit (Millipore). Briefly, chop tissue into small pieces (1–2 mm<sup>2</sup>) with a razor blade or scalpel. Transfer tissue into a tube with a screw cap lid and add formaldehyde to a final concentration of 1% and rotate tube at room temperature for 10 min. Chromatin was prepared by re-suspending fixed tissue pellet in tissue lysis buffer supplied by the vendor and sonicated to 200–500 bp. ChIP reactions (100 µg/reaction) were performed with the antibodies (5 µg/reaction) as listed in Table S1. Precipitated DNA–protein complexes were washed sequentially with RIPA buffer (50 mmol/L Tris, pH 8.0, 150 mmol/L NaCl, 0.1% SDS, 0.5% deoxycholate, 1% Nonidet P-40, 1 mmol/L EDTA), high salt buffer (50 mmol/L Tris, pH 8.0, 500 mmol/L NaCl, 0.1% SDS, 0.5% deoxycholate, 1% Nonidet P-40, 1 mmol/L EDTA), LiCl buffer (50 mmol/L Tris, pH 8.0, 250 mmol/L LiCl, 0.1% SDS, 0.5% deoxycholate, 1% Nonidet P-40, 1 mmol/L EDTA), and TE buffer (10 mmol/L Tris, 1 mmol/L EDTA pH 8.0), respectively. DNA–protein cross-link was reversed by heating the samples to 65 °C overnight. Proteins were digested with proteinase K (Sigma), and DNA was phenol/chloroform-extracted and precipitated by 100% ethanol. Dried DNA was dissolved in 50 µL of deionized distilled water and amplified with qPCR.

## 2.9. Human ALF specimens

Liver biopsies were collected from patients with ALF referring to Nanjing Drum Tower Hospital (Nanjing, China). Written informed consent was obtained from subjects or families of liver donors. All procedures that involved human samples were approved by the Ethics Committee of the Nanjing Drum Tower Hospital and adhered to the principles outlined in the Declaration of Helsinki. Paraffin sections were stained with indicated antibodies. Patient information is summarized in the Supporting Information Table S2.

## 2.10. Statistical analysis

One-way ANOVA with *post hoc* Scheffe analyses was performed by SPSS software (IBM SPSS v18.0, Chicago, IL, USA). Unless otherwise specified, values of *P* < 0.05 are considered statistically significant.

# 3. Results

## 3.1. MKL1 is activated in proliferating hepatocytes

To verify whether there might be a correlation between MKL1 and proliferation of hepatocytes, the following experiments were performed. Quantitative PCR (Fig. 1A) and Western blotting (Fig. 1B) showed that MKL1 expression was markedly up-regulated in the murine liver at 12, 24, and 48 h following partial hepatectomy (2/3) paralleling the induction of proliferative gene cyclin A2 (*Ccna2*). Similarly, MKL1 expression was also up-regulated in the murine livers following injection of acetaminophen (APAP), which is known to cause severe hepatic necrosis followed by liver regeneration (Fig. 1D and E). Immunohistochemical staining confirmed that up-regulation of MKL1 expression paralleled hepatocyte

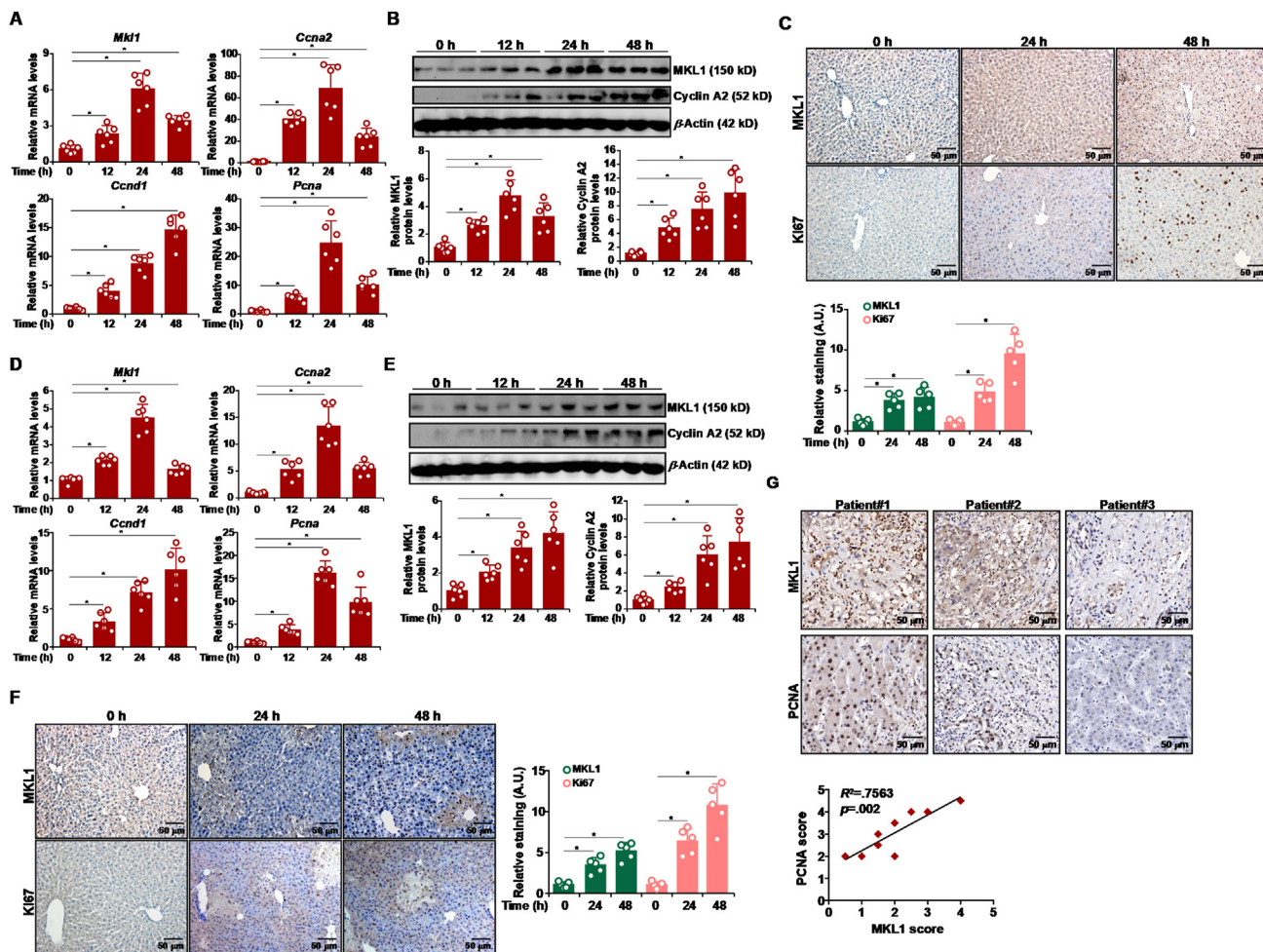


**Figure 1** (A–C) C57/B6 mice were subjected to 2/3 partial hepatectomy and sacrificed at indicated time points post-surgery. MKL1 expression levels in the liver were examined by qPCR and Western. Paraffin sections were stained with anti-MKL1 and anti-Ki67.  $n = 5–6$  mice for each group. Scale bar, 50  $\mu$ m. (D–F) C57/B6 mice were injected with APAP (300 mg/kg) and sacrificed at indicated time points post-injection. MKL1 expression levels in the liver were examined by qPCR and Western.  $n = 6$  mice for each group. Paraffin sections were stained with anti-MKL1 and anti-Ki67.  $n = 5–6$  mice for each group. Scale bar, 50  $\mu$ m. (G) Paraffin sections of liver specimens collected from patients with acute liver failure were stained with anti-MKL1 and anti-PCNA. Scale bar, 50  $\mu$ m.  $n = 9$  cases.

proliferation during liver regeneration induced by either liver resection or APAP injection (Fig. 1C and F). Treatment with the pro-proliferative stimuli HGF or Wnt3a resulted in robust induction of MKL1 (Supporting Information Fig. S1A and S1B). In order to tackle the question whether pro-regenerative stimuli regulated MKL1 expression at the transcriptional level, an *MKL1* promoter-luciferase construct<sup>35</sup> was transfected into HepG2 cells. Treatment with either HGF or Wnt3a robustly augmented the *MKL1* promoter activity (Supporting Information Fig. S2A). Ingenuity pathway analysis (IPA) identified several transcription factors that might contribute to *MKL1* trans-activation (Fig. S2B). A conserved NFAT4 consensus motif was located to the *MKL1* promoter, the mutation of which completely abrogated the induction by HGF/Wnt3a (Fig. S2C). As corroborating evidence, NFAT4 knockdown attenuated the up-regulation of MKL1 expression in hepatocytes exposed to HGF/Wnt3a treatment (Supporting Information Fig. S3). Furthermore, ChIP assay confirmed that NFAT4 could directly bind to the *MKL1* promoter in HGF/Wnt3a-treated hepatocytes *in vitro* and in the regenerating murine livers (Supporting Information Fig. S4). In addition, HGF or Wnt treatment promoted the migration of MKL1 into the

nucleus (Supporting Information Fig. S5). Finally, IHC analysis of human biopsy specimens collected from acute liver failure (ALF) patients (Fig. 1G) revealed that there was a positive correlation between MKL1 levels and hepatocyte proliferation. Taken together, these data suggest that augmented MKL1 activity correlates with liver regeneration.

### 3.2. Systemic *MKL1* deficiency retards liver regeneration

To directly probe the role of MKL1 in liver regeneration, MKL1 knockout (KO) mice and wild type (WT) littermates were subjected to 2/3 partial hepatectomy. Liver regeneration, as measured by liver weight versus body weight ratio, was slower in the MKL1 KO mice than in the WT mice. In accordance, MKL1 deficiency dampened the expression of several well-documented pro-proliferative genes in the liver (Fig. 2B and C). Immunohistochemical staining confirmed that proliferation (Ki67) and DNA replication (BrdU) of hepatocytes were less robust in the KO mice than in the WT mice (Fig. 2D). Similar observations were made in the pre-clinical model of liver failure in which the mice were subjected to lethal (4/5) hepatectomy (Fig. 2E–I).

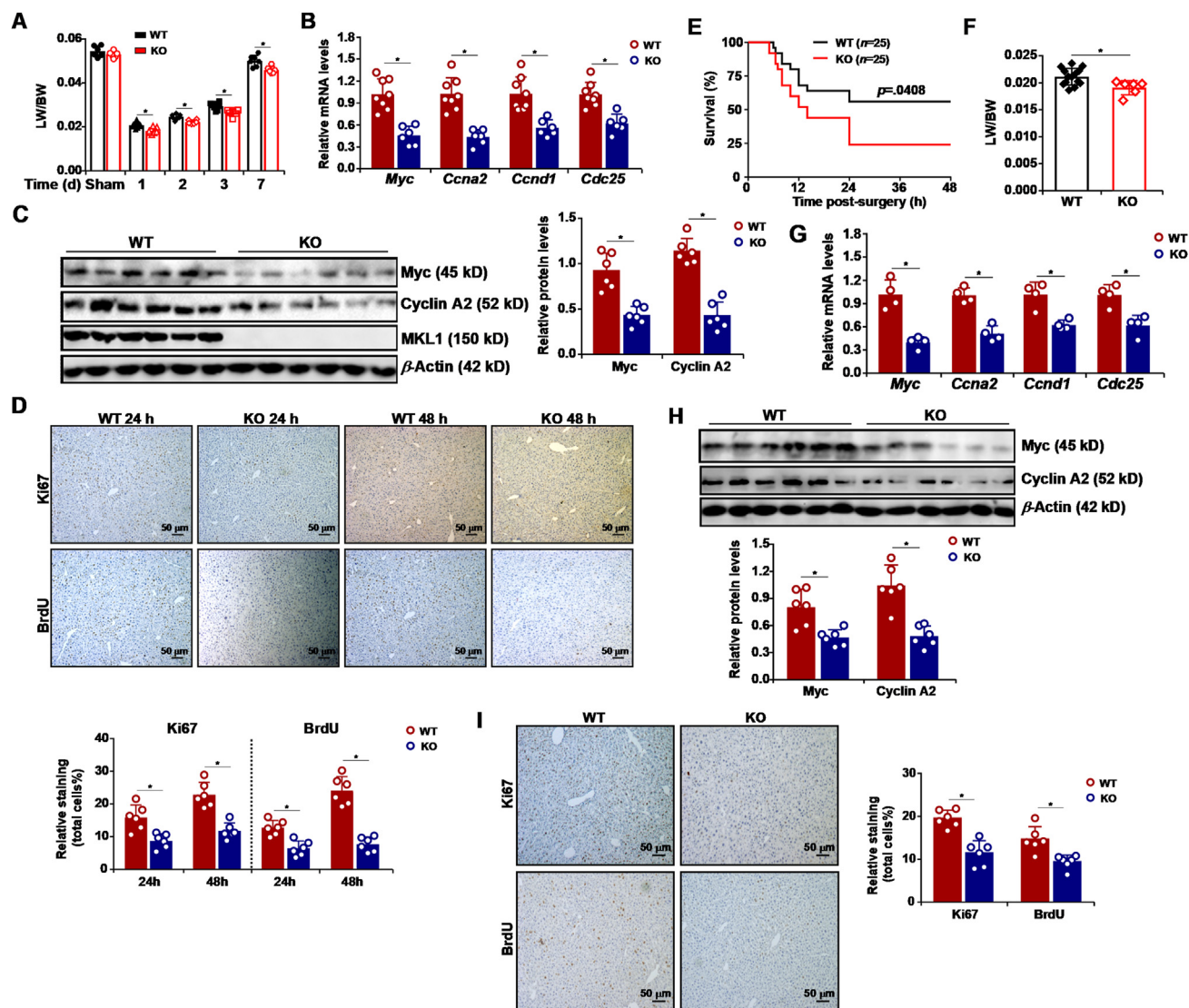


**Figure 2** Systemic MKL1 deletion impedes liver regeneration following partial hepatectomy in mice. (A–D) MKL1 knockout mice and the control mice were subjected to 2/3 partial hepatectomy. The mice were sacrificed at indicated time points post-surgery. Liver weight versus body weight ratios (A). Expression levels of pro-proliferative genes were examined by qPCR (B) and Western blot (C) one day after the surgery. Paraffin sections were stained with anti-Ki67 and anti-BrdU and quantified by Image Pro (D). Scale bar, 50  $\mu$ m. (E–I) WT and MKL1 KO mice were subjected to 4/5 partial hepatectomy. The mice were monitored for survival for 48 h after the surgery. Long-rank test was performed to determine statistical significance of survival (E). Expression levels of pro-proliferative genes were examined by qPCR (G) and Western blot (H). Paraffin sections were stained with anti-Ki67 and anti-BrdU and quantified by Image Pro (I). Scale bar, 50  $\mu$ m \* $P$  < 0.05 (two-tailed student's  $t$  test).

We next attempted to verify the role of MKL1 in liver regeneration in an alternative animal model in which the mice received a single injection of APAP. MKL1 deficiency aggravated liver injury and dampened liver regeneration in both the non-lethal APAP (300 mg/kg) model (Supporting Information Fig. S6) and the lethal APAP (800 mg/kg) model (Supporting Information Fig. S7). Together, these data suggest that MKL1 is essential for liver regeneration in mice.

### 3.3. Liver specific MKL1 deletion impedes liver regeneration

Because expansion of the hepatocyte population is key to liver regeneration, we asked whether MKL1 deletion in hepatocytes would similarly impact liver regeneration. *Mkl1<sup>fl/fl</sup>* mice were

crossed to the *Alb-Cre* mice to generate liver specific MKL1 knockout mice (*Alb-Cre; Mkl1<sup>fl/fl</sup>*, LKO). When 2/3 hepatectomy was performed in both the LKO mice and the control mice (*Mkl1<sup>fl/fl</sup>*), the LKO mice displayed a consistently smaller liver weight versus body weight ratio than the control mice (Fig. 3A). The defect in liver regeneration observed in the LKO mice was further verified by the analysis of pro-proliferative gene expression (Fig. 3B and C) and the quantification of Ki67<sup>+</sup>/BrdU<sup>+</sup> hepatocytes (Fig. 3D).

When these mice were subjected to 4/5 hepatectomy, a significantly larger fraction of the LKO mice succumbed to the loss of liver parenchyma (Fig. 3E). The remaining LKO mice exhibited retarded liver regeneration, as indicated by smaller liver weight versus body weight ratio (Fig. 3F), decreased expression of pro-proliferative

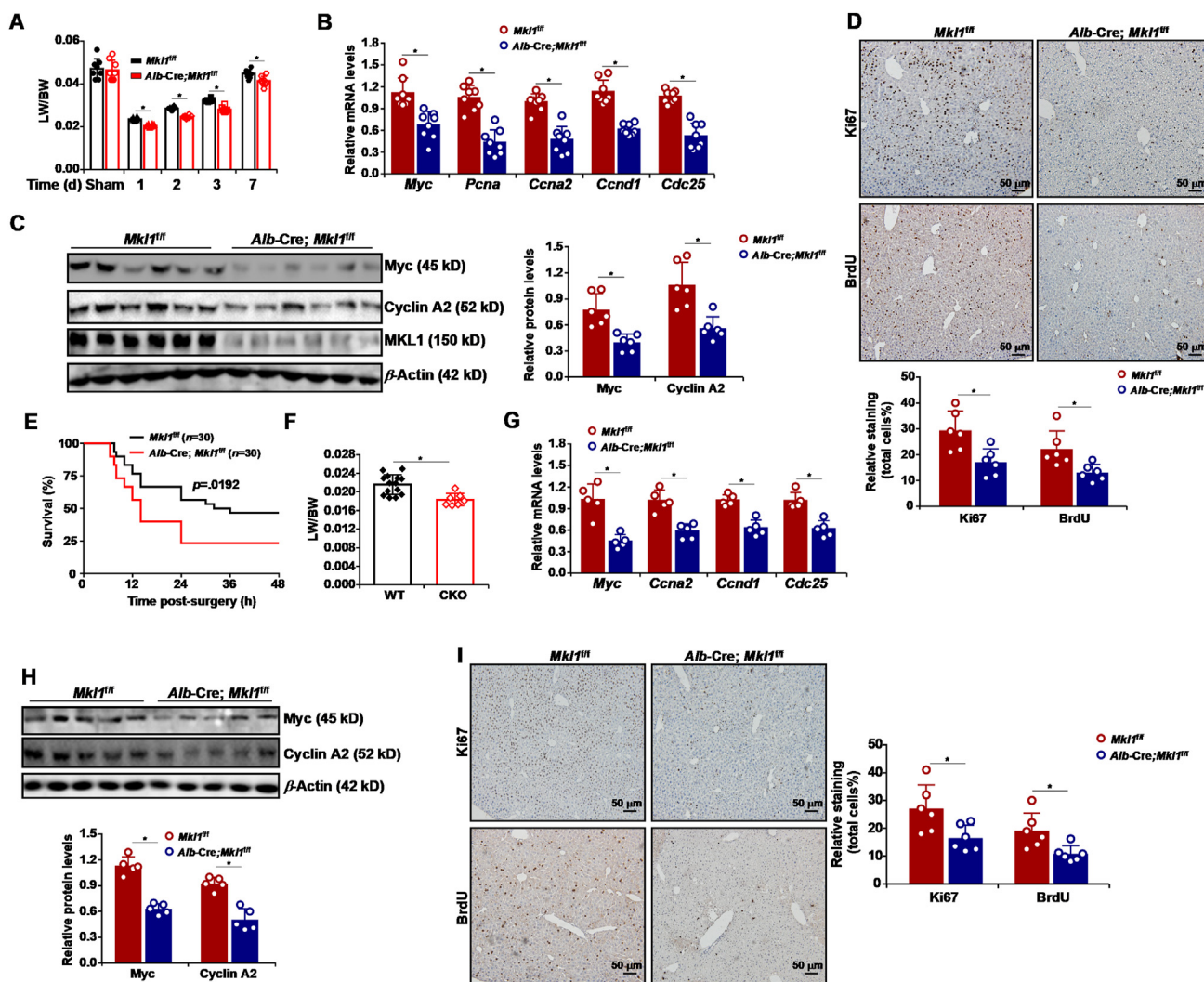


**Figure 3** Liver specific MKL1 deletion impedes liver regeneration following partial hepatectomy in mice. (A–D) WT (*Mkl1<sup>fl/fl</sup>*) and MKL1 LKO mice (*Alb-Cre; Mkl1<sup>fl/fl</sup>*) were subjected to 2/3 partial hepatectomy. The mice were sacrificed at indicated time points post-surgery. Liver weight *versus* body weight ratios (A). Expression levels of pro-proliferative genes were examined by qPCR (B) and Western blot (C) one day after the surgery. Paraffin sections were stained with anti-Ki67 and anti-BrdU and quantified by Image Pro (D). Scale bar, 50  $\mu$ m. (E–I) WT (*Mkl1<sup>fl/fl</sup>*) and MKL1 LKO mice (*Alb-Cre; Mkl1<sup>fl/fl</sup>*) were subjected to 4/5 partial hepatectomy. The mice were monitored for survival for 48 h after the surgery. Long-rank test was performed to determine statistical significance of survival (E). Expression levels of pro-proliferative genes were examined by qPCR (G) and Western blot (H). Paraffin sections were stained with anti-Ki67 and anti-BrdU and quantified by Image Pro (I). Scale bar, 50  $\mu$ m \* $P$  < 0.05 (two-tailed student's  $t$  test).

genes (Supporting Information Fig. S10A and S10B), and reduced Ki67<sup>+</sup>/BrdU<sup>+</sup> hepatocytes in the liver (Fig. S10C). Similar observations were made in the alternative model of liver regeneration post-APAP injection: in both the non-lethal (Supporting Information Fig. S11) and lethal (Supporting Information Fig. S12) APAP injection models, MKL1 deficiency in hepatocytes exacerbated liver injury and dampened liver regeneration. Combined, these data suggest that the ability of MKL1 to regulate liver regeneration is likely hepatocyte-autonomous.

### 3.4. Transcriptomic analysis points to MKL1 as a coordinator of liver regenerative response

We next evaluated the contribution of MKL1 to alteration of genomewide transcription during liver regenerative response. Liver tissues dissected from the WT and CKO mice 24 h after PHx. RNA-

seq showed that MKL1 deficiency resulted in more genes being down-regulated (163) than up-regulated (19) consistent with its role as a transcriptional activator (Fig. 4A). Most genes influenced by MKL1 deficiency appeared to be primarily involved in the regulation of cell cycling (Fig. 4B–D). HOMER analysis indicated that MKL1 deletion might negatively impact the activity of such transcription factors as NF- $\kappa$ B, E2F1 and GATA1 but boost the activity of ELF3, SMAD, and RAR $\alpha$  (Fig. 4E).

The same set of tissue samples were then subjected to ATAC-seq. As shown in Fig. 4F, chromatin accessibility in the proliferating hepatocytes was markedly altered in the absence of MKL1. GO and KEGG analysis of chromatin sites with altered accessibility highlighted that the processes related to cell cycling/proliferation were among the most prominently targeted by MKL1 (Fig. 4G). Indeed, increased chromatin “openness” was found to be correlated with induction of loci-specific gene expression

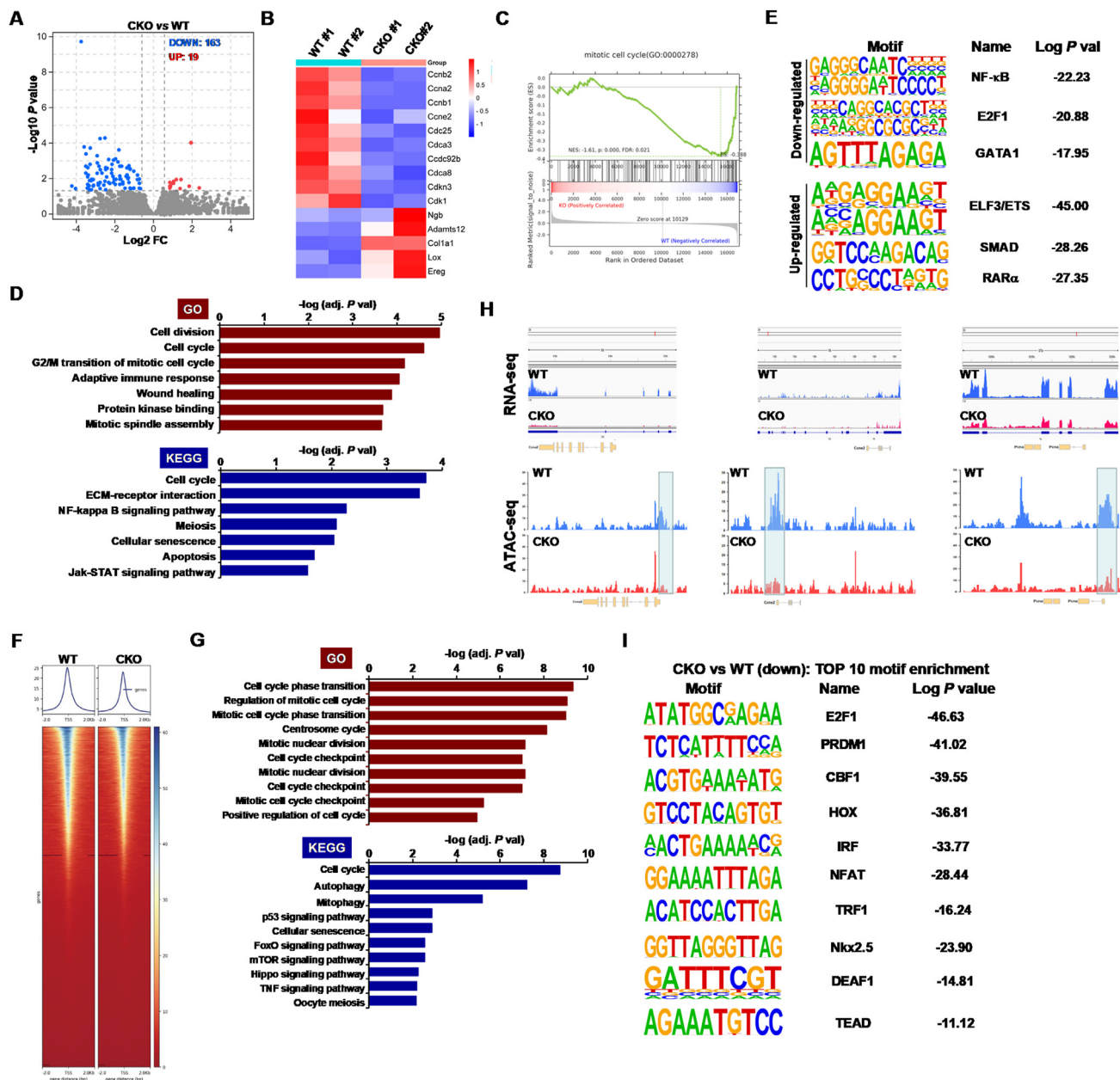


**Figure 4** MKL1 deficiency alters hepatic transcriptome following partial hepatectomy. (A–E) Hepatocyte conditional MKL1 knockout mice and the control mice were subjected to 2/3 partial hepatectomy. The mice were sacrificed 24 h after the surgery. RNA-seq was performed as described in Methods. Volcano plot (A). Heatmap of differentially expressed genes (B). GESA (C). GO and KEGG analysis of differentially expressed genes (D). HOMER analysis of differentially expressed genes (E). (F–I) Hepatocyte conditional MKL1 knockout mice and the control mice were subjected to 2/3 partial hepatectomy. The mice were sacrificed 24 h after the surgery. ATAC-seq was performed as described in Methods. Heatmap showing altered chromatin accessibility (F). GO and KEGG analysis (G). Representative RNA-seq and ATAC-seq peaks (H). HOMER analysis (I).

(Fig. 4H). Motif enrichment analysis indicated that MKL1-dependent sites may be targeted several sequence-specific transcription factors where E2F1 was on the top of the list (Fig. 4I).

3.5. MKL1 interacts with E2F1 to potentiate E2F1-dependent transcription

The evidence provided by our RNA-seq and ATAC-seq data that MKL1 might contribute to liver regeneration by modulating E2F1-dependent transcription prompted us to investigate the

mechanism underlying the MKL1–E2F1 interplay. HGF treatment up-regulated E2F1 activity robustly in WT hepatocytes but much less so in MKL1-null hepatocytes (Fig. 5A). Co-IP showed that much stronger interaction between MKL1 and E2F1 could be detected in the regenerating livers (PHx) than in the quiescent livers (Sham) (Fig. 5B). Re-ChIP assay further showed that stronger MKL1–E2F1 could be detected on several E2F1 target promoters during liver regeneration (Fig. 5C). To circumvent this issue that the above observations could be attributed to the increased availability of MKL1/E2F1 protein molecules rather

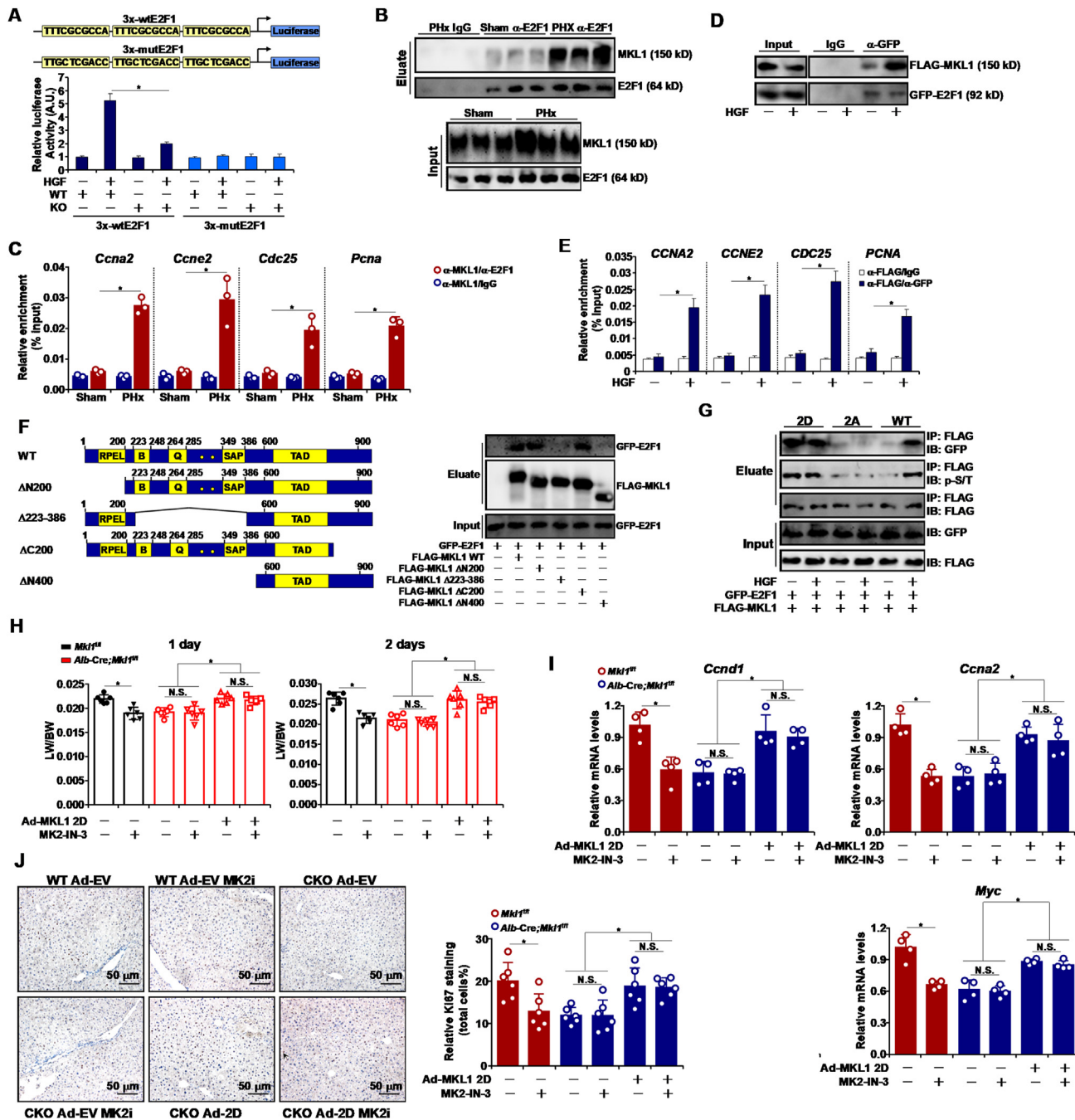


**Figure 5** MK2 contributes to liver regeneration through MKL1 phosphorylation. (A) WT or mutant E2F1 reporter was transfected into primary hepatocytes from WT or MKL1-KO mice followed by treatment with HGF for 12 h. Luciferase activities were normalized by GFP fluorescence and protein concentration. (B) Immunoprecipitation was performed with anti-E2F1 or pre-immune IgG using liver lysates from the mice subjected to PHx or the control mice. (C) Re-ChIP assay was performed with indicated antibodies using liver lysates from the mice subjected to PHx or the control mice. (D) HepG2 cells were transfected with adenovirus carrying FLAG-MKL1 and GFP-E2F1 followed by treatment with HGF (20 ng/mL). Immunoprecipitation was performed with anti-GFP or pre-immune IgG. (E) HepG2 cells were transfected with adenovirus carrying FLAG-MKL1 and GFP-E2F1 followed by treatment with HGF (20 ng/mL). Re-ChIP assay was performed with indicated antibodies. (F) HEK293 cells were transfected with indicated expression constructs. Immunoprecipitation was performed with anti-GFP. (G) HepG2 cells were transfected with FLAG-MKL1 and GFP-E2F1 in the presence or absence of HGF treatment. Immunoprecipitation was performed with anti-FLAG. (H–J) WT and MKL1 KO mice were injected with tail vein adenovirus carrying either MKL1 2D expression vector or an empty vector. Two weeks after viral injection, the mice were subjected to 2/3 PHx; 2 h prior to the surgery, the MK2 inhibitor was given orally at 20 mg/kg. Liver weight versus body weight ratio at 24 and 48 h after the surgery (H). Hepatic gene expression levels were measured by qPCR at 48 h after the surgery (I). Paraffin sections were stained with anti-Ki67 at 48 h after the surgery (J). Scale bar, 50  $\mu$ m.

than stronger MKL1–E2F1 interaction *per se*, adenovirus carrying exogenous, tagged MKL1 and E2F1 was used to transduce HepG2 cells; exposure to HGF treatment markedly enhanced the interaction between ectopically expressed MKL1 and E2F1 as evidenced by co-IP (Fig. 5D) and Re-ChIP (Fig. 5E) assays. Co-IP experiments performed to map the specific region(s) within MKL1 that might mediate its interaction with E2F1 indicated that whereas deletion of either the most N-terminus ( $\Delta$ N200) or the most C-terminus ( $\Delta$ C200) of MKL1 did not influence the interaction, deletion of the first 400 amino acids ( $\Delta$ N400) or combined deletion of the basic domain (B), the glutamine-rich domain (Q), and SAP domain ( $\Delta$ 223–386) completely abrogated the interaction (Fig. 5F).

### 3.6. MK2-mediated phosphorylation primes MKL1 for its interaction with E2F1

Based on these data, we hypothesized that a regeneration-sensitive switch within the MKL1 (*e.g.*, post-translational modification) might be responsible for the MKL1–E2F1 interaction. A previous report by Ronkina *et al.*<sup>36</sup> points to two serine residues, S351 and S371 located to the B/Q/SAP region that may be subject to stress-induced phosphorylation by MK2. Over-expression of a constitutive MK2 (MK2-EE) potentiated the E2F1 activity in wild type but not in MKL1-null hepatocytes (Fig. S11A). Similarly, over-expression of a dominant negative MK2 (MK2-KR) repressed HGF-induced E2F1 activity in wild type but not in MKL1-null hepatocytes suggesting that MK2 likely functions to modulate E2F1 activity through MKL1. Indeed, HGF treatment led to augmentation of MKL1 phosphorylation and enhanced interaction with E2F1, both of which was disrupted by MK2 knockdown (Fig. S11B). MK2 knockdown also blocked recruitment of MKL1 to the E2F1 target promoters without altering the binding of E2F1 itself (Fig. S11C). Likewise, treatment with an MK2 inhibitor (MK2-IN-3, MK2i) largely erased induction of MKL1 phosphorylation by HGF and intercepted its interaction with E2F1 (Fig. S11D). Again, ChIP assay confirmed that disruption of the MKL1–E2F1 interaction by MK2i treatment weakened MKL1 recruitment to the E2F1 target promoters without altering E2F1 binding (Fig. S11E). Importantly, substitution of S351/S371 with non-phosphorylatable alanines (2A) rendered MKL1 irresponsive to HGF-induced phosphorylation and E2F1 interaction whereas a constitutively phosphorylated mimetic (2D) displayed strong interaction with E2F1 in the absence of HGF (Fig. 5G).

### 3.7. MK2 contributes to liver regeneration through MKL1 phosphorylation

We then tackled the question as to whether MK2 might contribute to liver regeneration by licensing MKL1 phosphorylation. To this end, adenovirus carrying a constitutively phosphorylated MKL1 mimetic (Ad-MKL1 2D) was exploited (Fig. S12A). MK2 inhibition attenuated HGF-induced pro-proliferative response in WT but not MKL1 CKO hepatocytes as evidenced by qPCR measurements of proliferation-related gene expression (Fig. S12B) and EdU incorporation (Fig. S12C). Next, WT and MKL1 CKO mice were injected with Ad-MKL1 2D or Ad-EV followed by partial hepatectomy. Administration of MK2i significantly dampened liver regeneration in WT mice; the CKO mice displayed a dampened regenerative response compared to the WT mice but otherwise resistant to MK2i administration (Fig. 5J). Over-expression of MKL1 2D in the CKO mice not only restored

liver regeneration but offset the inhibitory effect of MK2i administration.

### 3.8. *Pld2* regulates MKL1 nuclear translocation to promote liver regeneration

We observed that MKL1 nuclear enrichment was elevated during liver regeneration *in vitro* (Fig. S5) and *in vivo* (Fig. 1G). Nuclear translocation of MKL1 is emphatically regulated by cytoskeletal remodeling, *i.e.*, polymerization of G-actin into F-actin<sup>37</sup>. Ha *et al.*<sup>38</sup> have previously shown that phospholipase D (PLD) promotes actin polymerization by catalyzing the production of phosphatidic acid (PA). PLD2 levels, but not PLD1 levels, were up-regulated in the regenerating liver in mice (Supporting Information Fig. S13). Consistently, PLD2 depletion dampened proliferation of hepatocytes and blocked MKL1 nuclear accumulation (Fig. 6A–C). More importantly, it was observed that AAV8-mediated delivery of shRNA targeting *Pld2* significantly dampened liver regeneration in mice (Fig. 6D–F). RNA-seq analysis indicated that *Pld2* knockdown markedly altered transcriptomics of hepatocytes (Fig. 6G and H). Of interest, *Pld2* deficiency was correlated with transcriptional programs involved in cell cycling (Fig. 6I) and dampened the activities of several pro-proliferative transcription factors including E2F1 (Fig. 6J).

### 3.9. PA promotes hepatocyte proliferation and rescues liver failure in a MKL1-dependent manner

HGF treatment significantly increased phosphatidic acid production in hepatocytes, which was completely abrogated by *Pld2* knockdown (Fig. 7A). On the contrary, PA treatment promoted hepatocyte proliferation in a dose-dependent manner (Supporting Information Fig. S14). However, response to PA was almost completely lost in MKL1-null hepatocytes (Fig. 7B and C). When both MKL1 CKO mice and WT mice were subjected to 4/5 PHx in a pre-clinical model of liver failure, PA administration significantly enhanced survival and promoted liver regeneration in WT, but not in MKL1 CKO, mice (Fig. 7D–G). RNA-seq analysis comparing the transcriptomes of hepatocytes exposed to PA or vehicle indicated that PA treatment altered the genes involved in cell proliferation augmented the activity of several pro-proliferative transcription factors including E2F1 (Fig. 7H–K).

### 3.10. PLD2-dependent PA synthesis is involved in liver regeneration in LF patients

Finally, the clinical relevance of our findings was validated in specimens from liver failure patients. As shown in Fig. 8A, *PLD2* expression levels were positively correlated with those of pro-regenerative genes, including *PCNA*, *CCNA2*, and *CCND1*, but inversely correlated with liver injury as gauged by plasma LDH levels. Similarly, it appeared that PA levels could be used to predict stronger hepatocyte proliferation and dampened liver injury (Fig. 8B). Therefore, we conclude that PLD2-dependent PA synthesis may be involved in liver regeneration in humans.

## 4. Discussion

Liver regeneration is a vastly complicated and highly coordinated pathophysiological process involving fundamental changes to the hepatocyte transcriptome<sup>8</sup>. Here we present a plethora body of

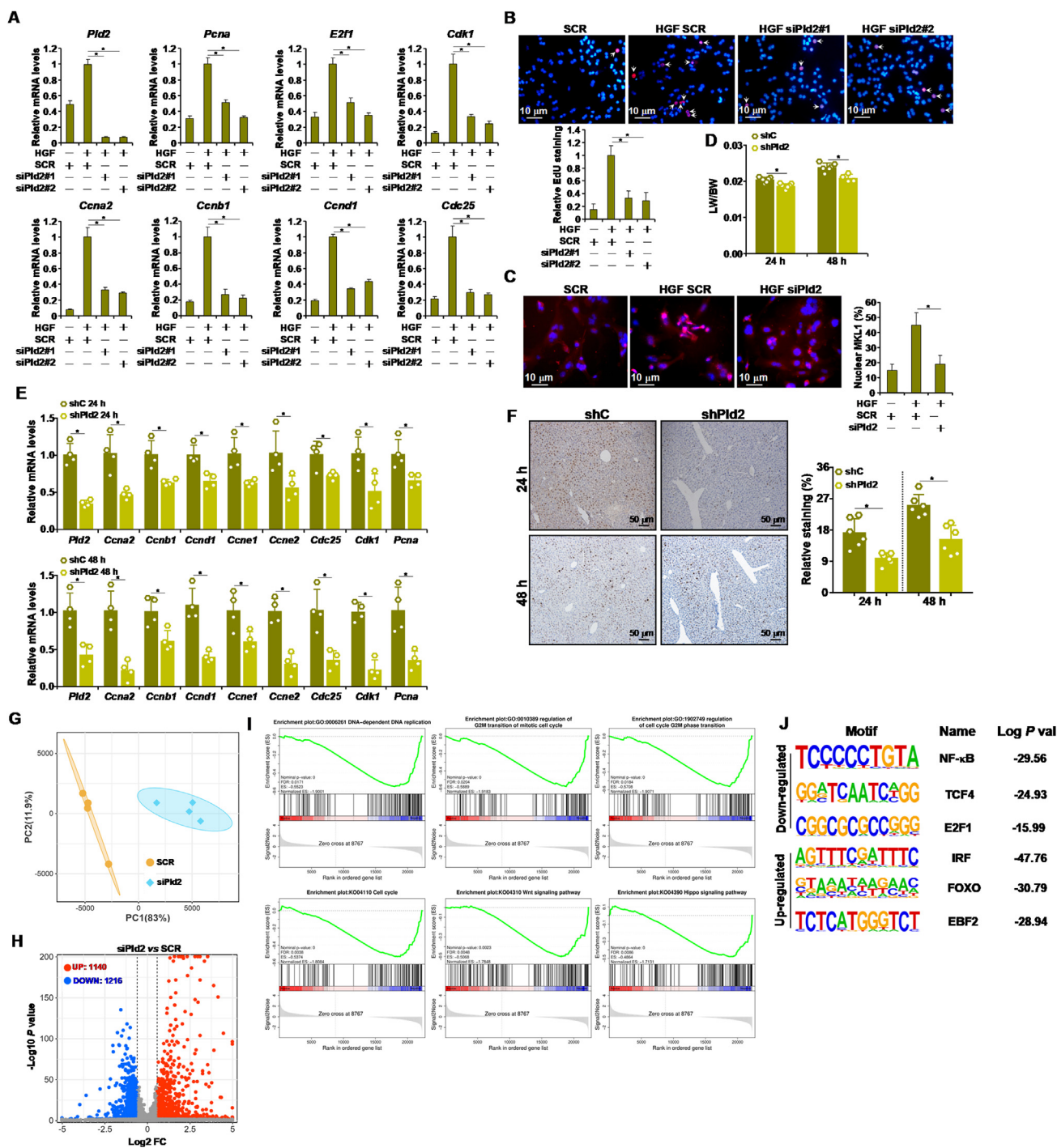


**Figure 6** PLD2 regulates MKL1 nuclear translocation to promote liver regeneration. (A–C) Primary hepatocytes were transfected with siRNAs targeting *Pld2* or scrambled siRNA (SCR) followed by treatment with HGF (20 ng/mL) for 24 h. Gene expression was examined by qPCR (A). Cell proliferation was examined by EdU incorporation (B). MKL1 localization was examined by immunofluorescence staining (C). (D–F) C57/B6 mice were injected with AAV8 carrying shRNA targeting *Pld2* (shPld2) or a control shRNA (shC). Two weeks after viral injection, the mice were subjected to 2/3 PHx. Liver weight *versus* body weight ratio at 24 and 48 h after the surgery (D). Hepatic gene expression levels were measured by qPCR at 48 h after the surgery (E). Paraffin sections were stained with anti-Ki67 at 48 h after the surgery (F). Scale bar, 50  $\mu$ m. (G–J) Primary hepatocytes were transfected with siRNAs targeting *Pld2* or SCR followed by treatment with HGF for 24 h. RNA-seq was performed as described in Methods. PCA plot (G). Volcano plot (H). GESA (I). HOMER analysis (J).

evidence to support a pivotal role for MKL1 in liver regeneration (Fig. 8C). We show here that MKL1 expression and activity (using its nuclear accumulation as a proxy) were responsive to pro-regenerative stimuli *in vivo* and *in vitro* and correlate with liver

regeneration in humans. Thus, MKL1 can be modified to tailor to the pro-regenerative reaction at least *via* two separate mechanisms. On the one hand, up-regulation of MKL1 expression, at the transcriptional level, is mediated by NFAT4. NFAT4 deficiency in mice has

been shown to impair liver regeneration without a clear explanation<sup>39</sup>. He et al.<sup>40</sup> and Charbonney et al.<sup>41</sup> have separately reported that the Wnt- $\beta$ -catenin pathway, a key promoter of liver regeneration, can augment MKL1 expression at transcriptional and post-transcriptional levels in epithelial cells. These observations appear to allude to a scenario wherein a panel of transcription factors converges on MKL1 to orchestrate pro-regenerative transcriptional programs. On the other hand, nuclear translocation of MKL1 is a well-studied process reliant on Rho-induced cytoskeletal remodeling<sup>37</sup>. Mounting evidence suggests that cytoskeletal re-contraction, through mechanosensing, is a pivotal step in the liver regenerative response<sup>42</sup>. Many of the mechanotransduction regulators, including YAP/Hippo<sup>43</sup> and SRF<sup>44</sup>, are known for their interactions with MKL1. In addition, Rho GTPases have been noted for their essential roles in hepatocyte proliferation and liver regeneration. Of interest, exposure of hepatocytes to Wnt ligand triggers robust nuclear enrichment of MKL1. These data combined neatly knit MKL1 into a network of pro-regenerative signaling wherein its expression and activity are tightly controlled to tailor to the regenerative response.

Transcriptomic analyses by RNA-seq and ATAC-seq reveal that yet another regulatory layer rendered by MKL1 to promote liver regeneration is through genomewide chromatin remodeling. Motif enrichment points to multiple sequence-specific transcription factors (TFs) whose bindings to the chromatin are impacted by MKL1 deficiency. Whereas some, including E2F, NFAT, and TEAD, possess relatively well-characterized roles in liver regeneration, evidence that supports the contribution to this process is circumstantial at best for most of these TFs and awaits validating. ChIP assay confirmed that MKL1-mediated chromatin rewiring may facilitate the assembly of the pre-initiation complex. It is not immediately clear how MKL1 regulates loosening/opening of chromatin conformation. One possibility is that MKL1 may interact with and recruit epigenetic factors to modulate histone/DNA modifications and/or nucleosome positioning rendering chromatin more accessible to the basic transcriptional machinery. For instance, the chromatin remodeling protein BRG1 known for its interaction with MKL1 to regulate smooth muscle cell lineage differentiation, has been reported to promote liver regeneration<sup>45</sup>. One key observation in our study is that the loss of MKL1 appears to perpetually hamper the proliferative/regenerative potential of hepatocytes because the decrease in liver weight/body weight ratio caused by MKL1 deficiency is discernible as early as 24 h post-PHx when liver mass just starts to increase. The underlying mechanism is not entirely clear. Possibly the extensive interactions of MKL1 with transcription factors and epigenetic factors enable MKL1 to fundamentally influence regeneration-related transcriptional events.

Whereas the phenotypes of MKL1 deficient mice in liver regeneration could certainly be attributed to, at least in part, defective cell cycling/division, compromised proliferation of MKL1-null hepatocytes *per se* does not necessarily encompass the entire spectrum of MKL1-dependent transcription events to fully support liver regeneration. For instance, several pathways related to immune response were identified by our RNA-seq and ATAC-seq analyses. Single-cell sequencing has revealed several clusters of hepatocytes that may contribute to liver regeneration by selectively expression inflammation-related molecules (*e.g.*, C-C motif ligand chemokines)<sup>46</sup>. Previous investigations have established MKL1 as a prominent activator of pro-inflammatory transcription in multiple cell lineages. It is likely that MKL1 may contribute to liver regeneration by regulating the production of hepatocyte-derived

inflammatory mediators to modulate hepatic immune homeostasis. Alternatively, a long-held view is that liver regeneration is fueled by metabolic reprogramming in hepatocytes<sup>47</sup>. Recent studies have built strong support for MKL1 as an integral regulator of lipid and glucose metabolism<sup>48</sup>. Our RNA-seq and ATAC-seq analyses point to significant alterations of metabolic pathways in MKL1-null hepatocytes compared to WT hepatocytes suggesting that MKL1 may contribute to liver regeneration by skewing cellular metabolism. These possibilities clearly deserve further attention.

We show here that MKL1 interaction with E2F1 and likely its ability to regulate liver regeneration are enabled by MK2-mediated phosphorylation. MK2 has been implicated in liver regeneration although direct evidence is lacking. Tormos et al.<sup>49</sup> have shown that hepatocyte-specific deletion of p38 $\alpha$ , the kinase immediately upstream of MK2, leads to retarded hepatocyte growth with a concomitant down-regulation of MK2 phosphorylation (activity) in a model of chronic biliary cirrhosis. More recently, Tamura and colleagues, using an *in vitro* liver slice culture system, have shown that MK2 deficiency dampens hepatocyte proliferation owing to down-regulation of immediate early genes (IEGs) and failed G1-S transition<sup>50</sup>. Of note, MK2 may target substrates other than MKL1 to participate in liver regeneration<sup>51</sup>. A proteomic profiling of MK2 targets in the context of liver regeneration would help clarify this issue and provide novel mechanistic insights on the role of MK2 in this process.

The most exciting finding of the present study is that regulation of MKL1 nuclear accumulation through PLD2-dependent PA production might contribute to liver regeneration. This observation is consistent with a recent report by Clemens et al.<sup>52</sup> in which PA administration alleviated liver injury in mice injected with non-lethal doses of APAP (250–350 mg/kg). Of interest, according to Clemens et al.<sup>53</sup>, the anti-necrotic effects of PA appear to be dependent on IL-6 production. An alternative mechanism underlying PA-mediated liver regeneration proposed by the same group of investigators stipulates that PA may directly regulate phosphorylation of and thus deactivate GSK3 thereby liberating  $\beta$ -catenin to migrate into the nucleus and orchestrate a pro-regenerative transcriptional program. These two models are not at all exclusive because  $\beta$ -catenin has been shown to bind to the IL-6 promoter and activate IL-6 transcription<sup>54,55</sup>. Coincidentally, we and others have reported that MKL1 could also directly bind to the IL-6 promoter and activate IL-6 transcription<sup>56–58</sup>. In addition, a crosstalk between MKL1 and Wnt/ $\beta$ -catenin has long been noted in different cells<sup>59–61</sup>. Although it remains to be determined whether PA enables to MKL1 to activate IL-6 transcription or to modulate Wnt/ $\beta$ -catenin signaling to promote liver regeneration, our data provide a strong rationale for exploiting PA and/or screening small-molecule compounds similar to PA to boost MKL1 activity as a reasonable approach to treat acute liver failure.

Despite the advances proffered by our study, a few critical issues deserve cautious consideration. First, although we propose that boosting MKL1 activity may be considered as a plausible strategy to treat liver failure, the potential benefit has to be weighed against the risk of malignant transformation of hepatocytes. For instance, MKL1 has been shown to support the expansion of hepatocellular carcinoma cells<sup>62,63</sup>. Additionally, augmented MKL1 activity in hepatocytes enables intracellular communication with hepatic stellate cells and promote liver fibrosis<sup>64</sup>. These observations, which argue for suppressing, rather than boosting, MKL1 activity for the treatment of liver diseases, beg for the inevitable question as to whether MKL1 can

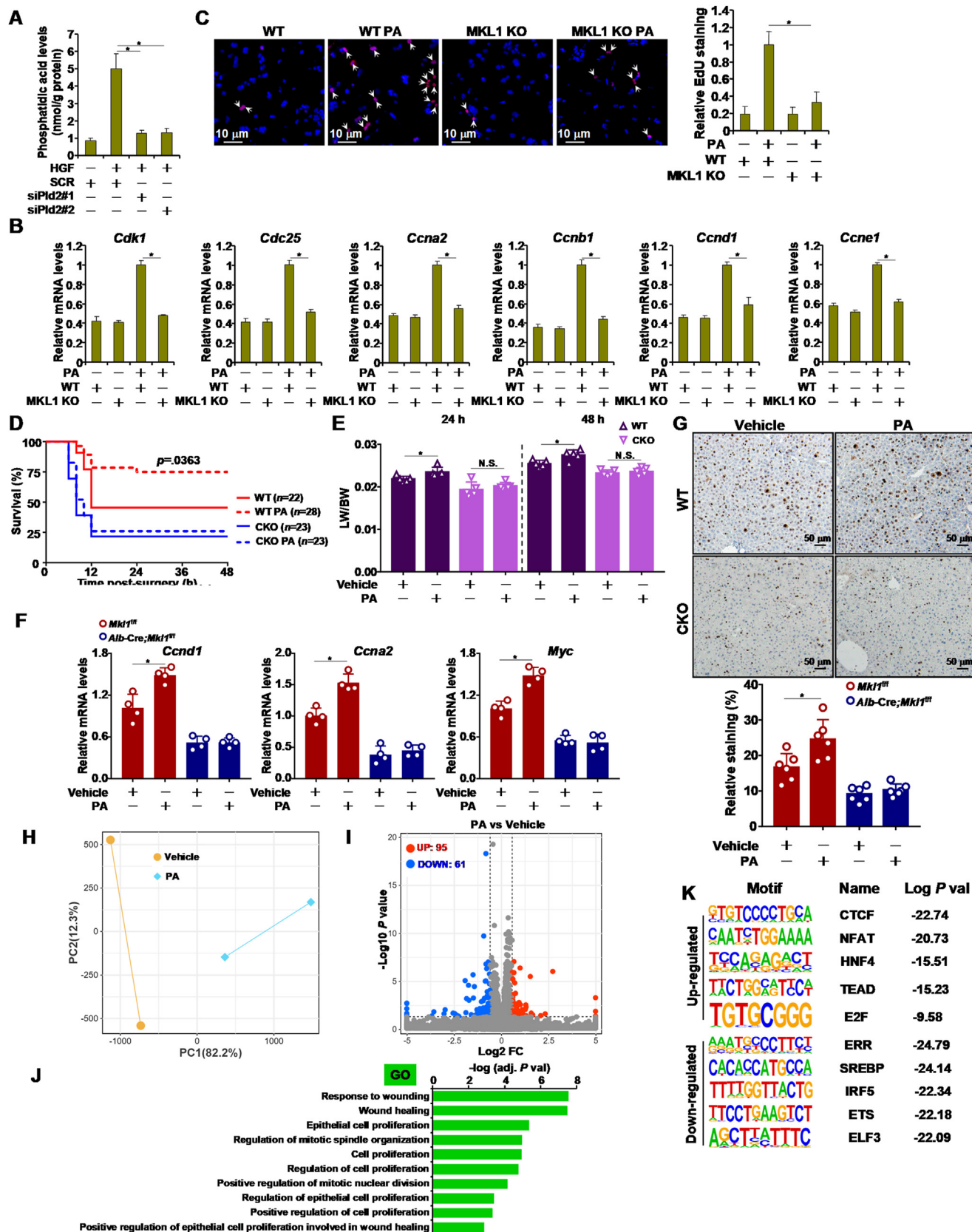


**Figure 7** PA promotes hepatocyte proliferation and rescues liver failure in a MKL1-dependent manner. (A) Primary hepatocytes were transfected with siRNAs targeting *Pld2* or SCR followed by treatment with HGF for 24 h. Intracellular PA levels were examined by ELISA. (B, C) Hepatocytes isolated from WT and MKL1 KO mice were exposed to PA (0.5  $\mu$ g/mL) for 24 h. Gene expression levels were examined by qPCR. Cell proliferation was examined by EdU. (D–G) 4/5 PHx was performed in WT and MKL1 CKO mice with or without PA injection (50 mg/kg).

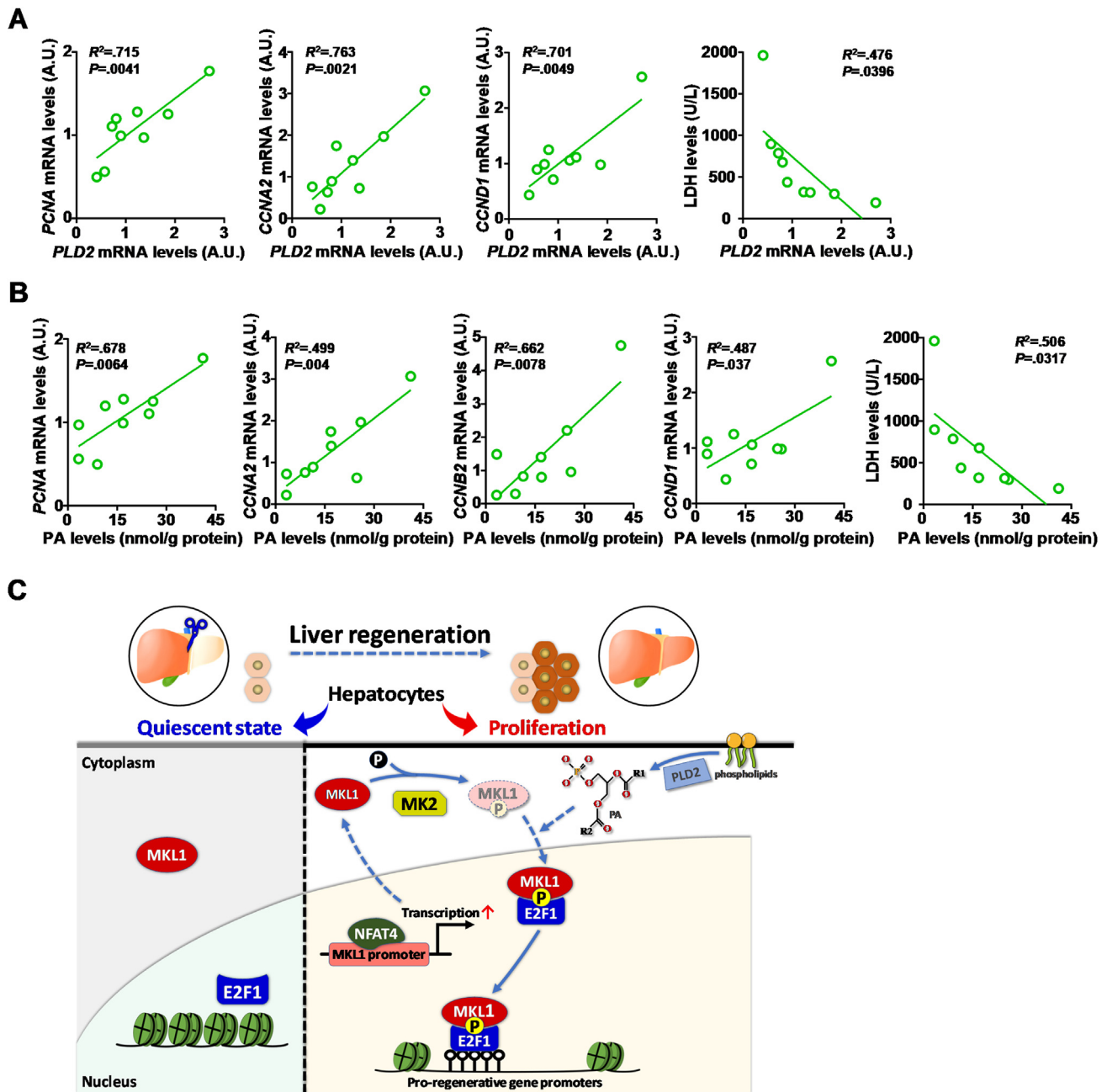


**Figure 8** PLD2-dependent PA synthesis is involved in liver regeneration in LF patients. (A) Correlation between hepatic PLD2 expression, expression of pro-proliferative genes, and plasma LDH levels in LF patients was determined by linear regression.  $n = 9$  cases. (B) Correlation between hepatic PA levels, expression of pro-proliferative genes, and plasma LDH levels in LF patients was determined by linear regression.  $n = 9$  cases. (C) A schematic model.

differentiate between the “benign” pro-proliferative signal, as in liver regeneration, and the “malignant” pro-proliferative signal, as in HCC development, and tailor specific transcription events to these different signals. Second, we focused on how MKL1 contributes to liver regeneration by regulating hepatocyte-autonomous

behavior. It should be noted that MKL1 is ubiquitously expressed and highly enriched in immune cells including macrophages (Kupffer cells) raising the intriguing possibility that MKL1 in non-parenchymal cells may play indispensable roles in liver regeneration. Although a role for macrophage-specific MKL1 in

The mice were monitored for 48 h after the surgery. Long-rank test was performed to determine statistical significance of survival (D). Body weight versus liver weight (E). Gene expression was examined by qPCR (F). Paraffin sections were stained with anti-Ki67 (G). Scale bar, 50  $\mu$ m. (H–K) Primary murine hepatocytes were exposed to PA (0.5  $\mu$ g/mL) or vehicle for 24 h. RNA-seq was performed as described in Methods. PCA plot (H). Volcano plot (I). GO analysis (J). HOMER analysis (K).

hepatic pathologies has yet to be demonstrated, previous investigations have shown that MKL1 deletion in macrophages mitigates tissue injury and/or promotes tissue repair in the heart<sup>25,65</sup>, the vasculature<sup>66</sup>, and the intestines<sup>57,67</sup>. It will be of great interest to determine whether mice harboring conditional MKL1 deletion in immune lineages display distinct phenotypes in models of liver injury and regeneration. Third, our findings in cultured cells and experimental animals only find limited support in humans due to the relatively small sample size and the heterogeneity of the specimens. Therefore, it remains to be determined whether MKL1 is universally essential for liver regeneration regardless of etiology or cue-dependent. These limitations notwithstanding, future studies should continue this line of investigation to develop novel therapeutics that are both effective and safe.

## 5. Conclusions

Our data reveal a novel mechanism whereby MKL1 contributes to liver regeneration. Screening for small-molecule compounds boosting MKL1 activity may be considered as a reasonable approach to treat acute liver failure.

## Acknowledgments

This work was supported by grants from the National Natural Science Foundation of China (82200684, 82121001, 81725001, and 81700554), and the Natural Science Foundation of Jiangsu Province (BK20221032).

## Author contributions

Yong Xu and Zilong Li conceived the project; Zilong Li and Jie Li designed experiments; Jiawen Zhou, Xinyue Sun, Xuelian Chen, Huimin Liu, Xiulian Miao, Yan Guo, and Zhiwen Fan performed experiments, collected data, and analyzed data; all authors wrote and edited the manuscript; Zilong Li, Zhiwen Fan, and Yong Xu secured funding.

## Conflicts of interest

The authors declare no conflicts of interest.

## Appendix A. Supporting information

Supporting data to this article can be found online at <https://doi.org/10.1016/j.apsb.2023.10.011>.

## References

1. Abu Rmilah A, Zhou W, Nelson E, Lin L, Amiot B, Nyberg SL. Understanding the marvels behind liver regeneration. *Wiley Interdiscip Rev Dev Biol* 2019;**8**:e340.
2. Fausto N, Campbell JS, Riehle KJ. Liver regeneration. *Hepatology* 2006;**43**:S45–53.
3. Forbes SJ, Newsome PN. Liver regeneration—mechanisms and models to clinical application. *Nature Rev Gastroenterol Hepatol* 2016;**13**:473–85.
4. Kurinna S, Barton MC. Cascades of transcription regulation during liver regeneration. *Int J Biochem Cell Biol* 2011;**43**:189–97.
5. Russell JO, Monga SP. Wnt/beta-catenin signaling in liver development, homeostasis, and pathobiology. *Annu Rev Pathol* 2018;**13**:351–78.
6. Moya IM, Halder G. Hippo-YAP/TAZ signalling in organ regeneration and regenerative medicine. *Nat Rev Mol Cell Biol* 2019;**20**:211–26.
7. Michalopoulos GK, Bhushan B. Liver regeneration: biological and pathological mechanisms and implications. *Nat Rev Gastroenterol Hepatol* 2021;**18**:40–55.
8. Wang AW, Wang YJ, Zahm AM, Morgan AR, Wangenstein KJ, Kaestner KH. The dynamic chromatin architecture of the regenerating liver. *Cell Mol Gastroenterol Hepatol* 2020;**9**:121–43.
9. Wang DZ, Li S, Hockemeyer D, Sutherland L, Wang Z, Schrott G, et al. Potentiation of serum response factor activity by a family of myocardin-related transcription factors. *Proc Natl Acad Sci U S A* 2002;**99**:14855–60.
10. Foster CT, Gualdrini F, Treisman R. Mutual dependence of the MRTF–SRF and YAP–TEAD pathways in cancer-associated fibroblasts is indirect and mediated by cytoskeletal dynamics. *Genes Dev* 2017;**31**:2361–75.
11. Xie L. MKL1/2 and ELK4 co-regulate distinct serum response factor (SRF) transcription programs in macrophages. *BMC Genom* 2014;**15**:301.
12. Scharenberg MA, Chiquet-Ehrismann R, Asparuhova MB. Megakaryoblastic leukemia protein-1 (MKL1): increasing evidence for an involvement in cancer progression and metastasis. *Int J Biochem Cell Mol* 2010;**42**:1911–4.
13. Brandt DT, Xu J, Steinbeisser H, Grosse R. Regulation of myocardin-related transcriptional coactivators through cofactor interactions in differentiation and cancer. *Cell Cycle* 2009;**8**:2523–7.
14. Muehlich S, Hampl V, Khalid S, Singer S, Frank N, Breuhahn K, et al. The transcriptional coactivators megakaryoblastic leukemia 1/2 mediate the effects of loss of the tumor suppressor deleted in liver cancer 1. *Oncogene* 2012;**31**:3913–23.
15. Hampl V, Martin C, Aigner A, Hoebel S, Singer S, Frank N, et al. Depletion of the transcriptional coactivators megakaryoblastic leukaemia 1 and 2 abolishes hepatocellular carcinoma xenograft growth by inducing oncogene-induced senescence. *EMBO Mol Med* 2013;**5**:1367–82.
16. Sun Y, Boyd K, Xu W, Ma J, Jackson CW, Fu A, et al. Acute myeloid leukemia-associated Mkl1 (Mrtf-a) is a key regulator of mammary gland function. *Mol Cell Biol* 2006;**26**:5809–26.
17. Wu T, Li N, Zhang Q, Liu R, Zhao H, Fan Z, et al. MKL1 fuels ROS-induced proliferation of vascular smooth muscle cells by modulating FOXM1 transcription. *Redox Biol* 2023;**59**:102586.
18. Li N, H L, Xue Y, Xu Z, Miao X, Guo Y, et al. Targetable Brg1–CXCL14 axis contributes to alcoholic liver injury by driving neutrophil trafficking. *EMBO Mol Med* 2023;**15**:e16592.
19. Fan Z, Kong M, Dong W, Dong C, Miao X, Guo Y, et al. Trans-activation of eotaxin-1 by Brg1 contributes to liver regeneration. *Cell Death Dis* 2022;**13**:495.
20. Jiang M, Guo R, Ai Y, Wang G, Tang P, Jia X, et al. Small molecule drugs promote repopulation of transplanted hepatocytes by stimulating cell dedifferentiation. *JHEP Rep* 2023;**5**:100670.
21. Sun Z, Wang Q, Sun L, Wu M, Li S, Hua H, et al. Acetaminophen-induced reduction of NIMA-related kinase 7 expression exacerbates acute liver injury. *JHEP Rep* 2022;**4**:100545.
22. Zhai T, Zhang J, Liu B, Zhou Z, Liu F, Wu Y. Cathelicidin promotes liver repair after acetaminophen-induced liver injury in mice. *JHEP Rep* 2023;**5**:100687.
23. Guo Y, Miao X, Sun X, Li L, Zhou A, Zhu X, et al. Zinc finger transcription factor Egf1 promotes non-alcoholic fatty liver disease. *JHEP Rep* 2023;**5**:100724.
24. Fan Z, Sun X, Chen X, Liu H, Miao X, Guo Y, et al. C–C motif chemokine CCL11 is a novel regulator and a potential therapeutic target in non-alcoholic fatty liver disease. *JHEP Rep* 2023;**5**:100805.

25. Liu L, Zhao Q, Kong M, Mao L, Yang Y, Xu Y. Myocardin-related transcription factor A regulates integrin beta 2 transcription to promote macrophage infiltration and cardiac hypertrophy in mice. *Cardiovasc Res* 2022;**118**:844–58.
26. Zhang W, Ji W, Liu X, Ouyang G, Xiao W. ELL inhibits E2F1 transcriptional activity by enhancing E2F1 deacetylation via recruitment of histone deacetylase 1. *Mol Cell Biol* 2014;**34**:765–75.
27. Wu X, Miao X, Guo Y, Shao T, Tang S, Lin Y, et al. Slug enables redox-sensitive trans-activation of LRP1 by COUP-TFII: implication in antifibrotic intervention in the kidneys. *Life Sci* 2023;121412.
28. Lei MML, Leung CON, Lau EYT, Leung RWH, Ma VWS, Tong M, et al. SCYL3, as a novel binding partner and regulator of ROCK2, promotes hepatocellular carcinoma progression. *JHEP Rep* 2023;**5**:100604.
29. Nalkurthi C, Schroder WA, Melino M, Irvine KM, Nyuydzefe M, Chen W, et al. ROCK2 inhibition attenuates profibrogenic immune cell function to reverse thioacetamide-induced liver fibrosis. *JHEP Rep* 2022;**4**:100386.
30. Kunst RF, de Waart DR, Wolters F, Duijst S, Vogels EW, Bolt I, et al. Systemic ASBT inactivation protects against liver damage in obstructive cholestasis in mice. *JHEP Rep* 2022;**4**:100573.
31. Su W, Gao W, Zhang R, Wang Q, Li L, Bu Q, et al. TAK1 deficiency promotes liver injury and tumorigenesis via ferroptosis and macrophage cGAS–STING signalling. *JHEP Rep* 2023;**5**:100695.
32. Seedorf K, Weber C, Vinson C, Berger S, Vuillard LM, Kiss A, et al. Selective disruption of NRF2–KEAP1 interaction leads to NASH resolution and reduction of liver fibrosis in mice. *JHEP Rep* 2023;**5**:100651.
33. Zhu B, Ni Y, Gong Y, Kang X, Guo H, Liu X, et al. Formononetin ameliorates ferroptosis-associated fibrosis in renal tubular epithelial cells and in mice with chronic kidney disease by suppressing the Smad3/ATF3/SLC7A11 signaling. *Life Sci* 2023;**315**:121331.
34. Jiao J, Sanchez JI, Saldarriaga OA, Solis LM, Twardy DJ, Maru DM, et al. Spatial molecular and cellular determinants of STAT3 activation in liver fibrosis progression in non-alcoholic fatty liver disease. *JHEP Rep* 2023;**5**:100628.
35. Kong M, Hong W, Shao Y, Lv F, Fan Z, Li P, et al. Ablation of serum response factor in hepatic stellate cells attenuates liver fibrosis. *J Mol Med (Berl)* 2019;**97**:1521–33.
36. Ronkina N, Lafera J, Kotlyarov A, Gaestel M. Stress-dependent phosphorylation of myocardin-related transcription factor A (MRTF-A) by the p38(MAPK)/MK2 axis. *Sci Rep* 2016;**6**:31219.
37. Olson EN, Nordheim A. Linking actin dynamics and gene transcription to drive cellular motile functions. *Nat Rev Mol Cell Biol* 2010;**11**:353–65.
38. Ha KS, Exton JH. Activation of actin polymerization by phosphatidic acid derived from phosphatidylcholine in IIC9 fibroblasts. *J Cell Biol* 1993;**123**:1789–96.
39. Pierre KB, Jones CM, Pierce JM, Nicoud IB, Earl TM, Chari RS. NFAT4 deficiency results in incomplete liver regeneration following partial hepatectomy. *J Surg Res* 2009;**154**:226–33.
40. He H, Du F, He Y, Wei Z, Meng C, Xu Y, et al. The Wnt–beta-catenin signaling regulated MRTF-A transcription to activate migration-related genes in human breast cancer cells. *Oncotarget* 2018;**9**:15239–51.
41. Charbonney E, Speight P, Masszi A, Nakano H, Kapus A. beta-Catenin and Smad3 regulate the activity and stability of myocardin-related transcription factor during epithelial–myofibroblast transition. *Mol Biol Cell* 2011;**22**:4472–85.
42. Song Z, Gupta K, Ng IC, Xing J, Yang YA, Yu H. Mechanosensing in liver regeneration. *Semin Cell Dev Biol* 2017;**71**:153–67.
43. Manmadhan S, Ehmer U. Hippo signaling in the liver—a long and ever-expanding story. *Front Cell Dev Biol* 2019;**7**:33.
44. Cho S, Irianto J, Discher DE. Mechanosensing by the nucleus: from pathways to scaling relationships. *J Cell Biol* 2017;**216**:305–15.
45. Li N, Kong M, Zeng S, Hao C, Li M, Li L, et al. Brahma related gene 1 (*Brg1*) contributes to liver regeneration by epigenetically activating the Wnt/beta-catenin pathway in mice. *FASEB J* 2019;**33**:327–38.
46. Chang N, Tian L, Ji X, Zhou X, Hou L, Zhao X, et al. Single-cell transcriptomes reveal characteristic features of mouse hepatocytes with liver cholestatic injury. *Cells* 2019;**8**:1069.
47. Caldez MJ, Van Hul N, Koh HWL, Teo XQ, Fan JJ, Tan PY, et al. Metabolic remodeling during liver regeneration. *Dev Cell* 2018;**47**:425–438.e5.
48. Sward K, Stenkula KG, Rippe C, Alajbegovic A, Gomez MF, Albinsson S. Emerging roles of the myocardin family of proteins in lipid and glucose metabolism. *J Physiol* 2016;**594**:4741–52.
49. Tormos AM, Arduini A, Talens-Visconti R, del Barco Barrantes I, Nebreda AR, Sastre J. Liver-specific p38alpha deficiency causes reduced cell growth and cytokinesis failure during chronic biliary cirrhosis in mice. *Hepatology* 2013;**57**:1950–61.
50. Tran DDH, Koch A, Saran S, Armbrecht M, Ewald F, Koch M, et al. Extracellular-signal regulated kinase (Erk1/2), mitogen-activated protein kinase-activated protein kinase 2 (MK2) and tristetraprolin (TTP) comprehensively regulate injury-induced immediate early gene (IEG) response in *in vitro* liver organ culture. *Cell Signal* 2016;**28**:438–47.
51. Morgan D, Berggren KL, Spiess CD, Smith HM, Tejwani A, Weir SJ, et al. Mitogen-activated protein kinase-activated protein kinase-2 (MK2) and its role in cell survival, inflammatory signaling, and migration in promoting cancer. *Mol Carcinog* 2022;**61**:173–99.
52. Clemens MM, Kennon-McGill S, Vazquez JH, Stephens OW, Peterson EA, Johann DJ, et al. Exogenous phosphatidic acid reduces acetaminophen-induced liver injury in mice by activating hepatic interleukin-6 signaling through inter-organ crosstalk. *Acta Pharm Sin B* 2021;**11**:3836–46.
53. Clemens MM, Kennon-McGill S, Apte U, James LP, Finck BN, McGill MR. The inhibitor of glycerol 3-phosphate acyltransferase FSG67 blunts liver regeneration after acetaminophen overdose by altering GSK3beta and Wnt/beta-catenin signaling. *Food Chem Toxicol* 2019;**125**:279–88.
54. Jang J, Ha JH, Chung SI, Yoon Y. Beta-catenin regulates NF-kappaB activity and inflammatory cytokine expression in bronchial epithelial cells treated with lipopolysaccharide. *Int J Mol Med* 2014;**34**:632–8.
55. Edara VV, Nooka S, Proulx J, Stacy S, Ghorpade A, Borgmann K. beta-Catenin regulates wound healing and IL-6 expression in activated human astrocytes. *Biomedicines* 2020;**8**:479.
56. Zhang M, Gao J, Zhao X, Zhao M, Ma D, Zhang X, et al. p38alpha in macrophages aggravates arterial endothelium injury by releasing IL-6 through phosphorylating megakaryocytic leukemia 1. *Redox Biol* 2021;**38**:101775.
57. Yu L, Weng X, Liang P, Dai X, Wu X, Xu H, et al. MRTF-A mediates LPS-induced pro-inflammatory transcription by interacting with the COMPASS complex. *J Cell Sci* 2014;**127**:4645–57.
58. Wan C, Liu W, Jiang L, Dong S, Ma W, Wang S, et al. Knockdown of MKL1 ameliorates oxidative stress-induced chondrocyte apoptosis and cartilage matrix degeneration by activating TWIST1-mediated PI3K/AKT signaling pathway in rats. *Autoimmunity* 2022;**55**:559–66.
59. Kumawat K, Koopmans T, Menzen MH, Prins A, Smit M, Halayko AJ, et al. Cooperative signaling by TGF-beta1 and WNT-11 drives sm-alpha-actin expression in smooth muscle via Rho kinase-actin-MRTF-A signaling. *Am J Physiol Lung Cell Mol Physiol* 2016;**311**:L529–37.
60. Taiyab A, Holms J, West-Mays JA. beta-Catenin/Smad3 interaction regulates transforming growth factor-beta-induced epithelial to mesenchymal transition in the lens. *Int J Mol Sci* 2019;**20**:2078.
61. Yin L, Liu T, Li C, Yan G, Zhang J, Wang L. The MRTF-A/miR-155/SOX1 pathway mediates gastric cancer migration and invasion. *Cancer Cell Int* 2020;**20**:303.
62. Liu Z, Sun J, Li C, Xu L, Liu J. MKL1 regulates hepatocellular carcinoma cell proliferation, migration and apoptosis via the COMPASS complex and NF-kB signaling. *BMC Cancer* 2021;**21**:1184.
63. Hermanns C, Hampl V, Holzer K, Aigner A, Penkava J, Frank N, et al. The novel MKL target gene myoferlin modulates expansion and senescence of hepatocellular carcinoma. *Oncogene* 2017;**36**:3464–76.

64. Li Z, Li P, Lu Y, Sun D, Zhang X, Xu Y. A non-autonomous role of MKL1 in the activation of hepatic stellate cells. *Biochim Biophys Acta Gene Regul Mech* 2019;**1862**:609–18.
65. Yu L, Yang G, Zhang X, Wang P, Weng X, Yang Y, et al. Megakaryocytic leukemia 1 (MKL1) bridges epigenetic activation of NADPH oxidase in macrophages to cardiac ischemia–reperfusion injury. *Circulation* 2018;**138**:2820–36.
66. An J, Naruse TK, Hinohara K, Soejima Y, Sawabe M, Nakagawa Y, et al. MRTF-A regulates proliferation and survival properties of pro-atherogenic macrophages. *J Mol Cell Cardiol* 2019;**133**:26–35.
67. An J, Nagaishi T, Watabe T, Naruse TK, Watanabe M, Kimura A. MKL1 expressed in macrophages contributes to the development of murine colitis. *Sci Rep* 2017;**7**:13650.